Physical Review & Research International
2(4): 133-143, 2012

SCIENCEDOMAIN *international*
www.sciencedomain.org

Elastic Torsion of Bars with "Pound" and "Yen" Cross Sections Using Large Singular Finite Element Method

Ouigou Michel Zongo[1*], Sié Kam[1], Péléga Florent Kieno[1] and Alioune Ouedraogo[1]

[1]Department of Physics, UFR-SEA, University of Ouagadougou, B.P 7021, Ouagadougou 03, Burkina Faso.

Authors' contributions

This work was carried out in collaboration between all authors. All authors read and approved the final manuscript.

Research Article

Received 18th July 2012
Accepted 21st October 2012
Published 12th December 2012

ABSTRACT

Aims: Solving Dirichlet's problem through large singular finite elements method for the Poisson's equation.
Study design: Large Singular Finite Elements Method (LSFEM).
Place and Duration of Study: Sample: Department of Physics, UFR-SEA, University of Ouagadougou, Burkina Faso, between September 2010 and July 2012.
Methodology: There are 3 steps for LSFE Method; After the decomposition of the domain in subdomains, we resolve auxiliary problems and connect auxiliary solutions, using MATLAB software.
Results: For each of both membranes, the minimum global error is $1.3\text{x}10^{-12}$. It is obtained at the twelfth approximation when $140 \times N = 1680$ coefficients a_{ki} are maintained as a whole. This suggests that the distorted u of the membrane can be determined with 13 or 14 significant digits, while its derivatives $\frac{\partial u}{\partial x}$ and $\frac{\partial u}{\partial y}$ may be calculated with 11 or 12 significant digits. These results are compared with those obtained through finite elements method. Both methods provide results that align quite well everywhere except near the singularities with significant differences.

Keywords: Large elements; least squares; finite elements; singularities.

[*]Corresponding author: Email: zongo@univ-ouaga.bf;

1. INTRODUCTION

The weak torsion of thin cylindrical bars allows solving Poisson's equation with homogeneous Dirichlet boundary conditions. It is assumed that the torsion occurs without any volume change, i.e. a deformation of pure sliding. In the case of polygonal bars, it is very difficult to deal with Poisson's equation numerically and the usual method of finite elements or finite differences provides poor results when used in their standard form. These methods as demonstrated by various authors: Barnill and Whiteman [1]; Emery [2]; Fix [3]; Motz [4]; Strang and Fix [5]; Wait and Mitchell [6], can be significantly improved if they take the analytical form of the solution near the singularities into account. Large singular finite elements method will be used to solve Poisson's equation.

2. PROBLEM TO SOLVE AND METHOD USED

Torsion of bars with polygonal section was studied using boundary collocation method, Kolodziej and Fraska [7] and using Trefftz integral for the complex torsion function, Hassenpflug [8].

For two years, we worked on the solutions of Dirichlet's problem Zongo et al. [9,10]. Present study deals with Dirichlet boundary conditions. We need to solve a Poisson's equation in the first isospectral plane domains discovered by reference Gordon et al. [11] with homogeneous Dirichlet boundary conditions. These domains are often known as "Pound" and "Yen" because they look like the corresponding currency symbols and are represented in Fig. 1. The equations of the torsion of a thin bar of cross section Ω as found in Landau and Lifshitz [12], Timoshenko and Goodier [13],

$$\Delta u(x,y) = -1 \ (x,y) \in \Omega \tag{1}$$

$$u(x,y) = 0 \ (x,y) \in \partial\Omega \tag{2}$$

Domains Ω of R^2 are the cross sections of bars which are Gordon, Webb and Wolpert membranes submitted to the torsion. The function u is a potential of constraints from which can be derived non-zero components (3) and (4) of the stress tensor at any point of the bar. As for $\partial\Omega$, it is the boundary of Ω domain.

$$\tau_{xz} = 2G\alpha \frac{\partial u}{\partial y} \tag{3}$$

$$\tau_{yz} = -2G\alpha \frac{\partial u}{\partial x} \tag{4}$$

Where G is the modulus of shear (sliding) fraction, α the unit torsion angle and z the axis, which, with x and y, makes a direct orthogonal reference with coordinate system.

From expressions (1) to (4) x and y are Cartesian coordinates of the point in the domain Ω. The problem as posed is singular with the twenty nine geometrical singularities which constitute the corners of the boundary of the domain. Such domains have no geometric symmetry that allows reducing the study domain (Fig. 1). We must therefore consider the 29-gons as a whole and solve it through large singular finite elements method.

Large singular finite elements method comprises three steps, reference Tolley [14]:

Step 1: Decomposition of the domain

The first step of the method gives the splitting up of both domains into as many subdomains as there are singularities; in the twenty-nine geometrical singularities, we added eight artificial singularities on the longer sides of the domain; each subdomain contains only one singularity. This splitting up will give for each of the domains, thirty seven subdomains Ω_j shown in red and separated by fifty two sub-boundaries Γ_{ij} comprising:

- Six identical rectangular trapezoids with angles measuring 3π / 4 radians
- Twelve squares of unit side
- Eleven L-shaped identical subdomains
- Eight rectangles which sides are respectively 2 and 1

The eleven L-shaped subdomain with 270º inside angles are the most severe singularities.

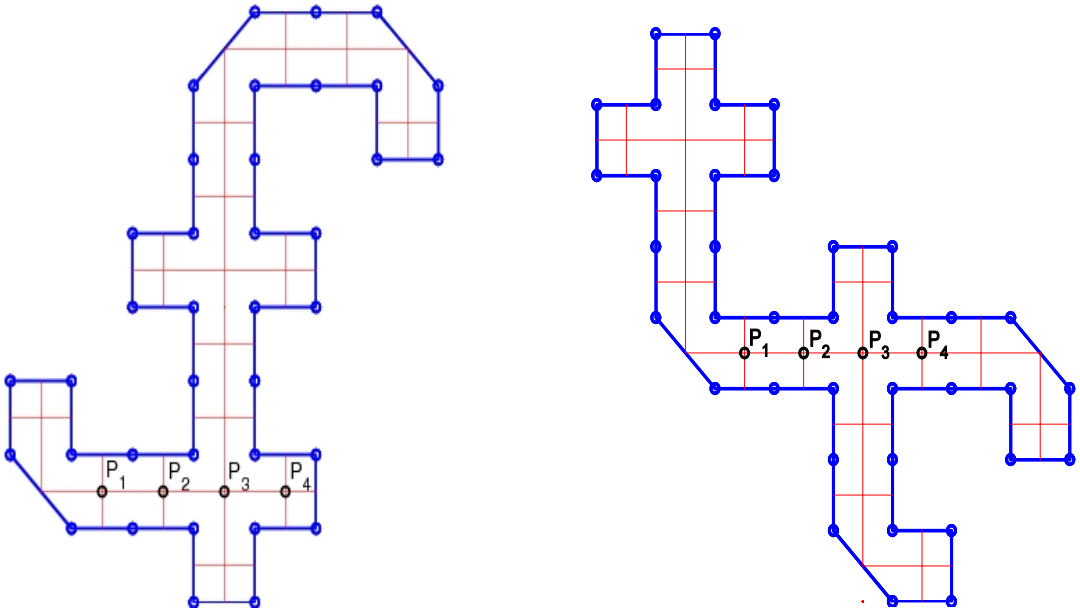

Fig. 1. Gordon, Webb, and Wolpert "Pound" and "Yen" isospectral domains. Decomposition into subdomains and alignment of reference points

The shortest sides of the domains have a reduced unit length and the longest sides have double length.

Step 2: Resolving auxiliary problems

Auxiliary problems are posed as there are auxiliary domains Ω_j. Therefore, to each subdomain Ω_j, is associated with an origin σ_j which is a singularity, an angle α_j which is the opening angle of the subdomain and a local system with polar coordinates (r_j, θ_j).

For each subdomain, the following auxiliary problem is solved:

$$\Delta u_j(r_j, \theta_j) = -1 \ (r_j, \theta_j) \in \Omega_j \tag{5}$$

$$u_j(r_j, 0) = 0 \tag{6}$$

$$u_j(r_j, \alpha_j) = 0 \tag{7}$$

with $j = 1, \ldots, 37$.

Solution of each auxiliary problem is not fully determined. Indeed, each problem is particular, because no constraint is put on u_i solution to infinite. It is possible to find an indefinite number of solutions. Broadly speaking, we can write functions $u_j(r_j, \theta_j)$ that solve equations (5) to (7) as Tolley [14,15]

$$u_j(r_j, \theta_j) = u_{j,p}(r_j, \theta_j) + \sum_{k=1}^{\infty} a_{jk} u_{jk,h}(r_j, \theta_j) \ (j = 1, \ 2, \ ..,37) \tag{8}$$

or $u_{j,p}$ is a particular solution to problems (6) to (7); $u_{jk,h}$ are solutions to the homogenous problems associated. Various auxiliary solutions per type of subdomain and boundary conditions are written as follow, Tolley [15]:

- As for the eleven L-shaped subdomains:

$$u_k(r_k, \theta_k) = \sum_{l=1}^{\infty} a_{kl} r_k^{\frac{2k}{3}} \sin(\frac{2l\theta_k}{3}) + \frac{r_k^2}{12\pi}[(3\pi - 4\theta_k)\cos 2\theta_k - 3\pi - 4\log r_k \sin 2\theta_k] \tag{9-a}$$

- As for square subdomains:

$$u_i(r_i, \theta_i) = \sum_{n=1}^{\infty} a_{in} r_i^{2n} \sin 2n\theta_i + \frac{r_i^2}{4\pi}[(\pi - 4\theta_i)\cos 2\theta_i - \pi - 4\log r_i \sin 2\theta_i] \tag{10-a}$$

- As for the eight rectangular subdomains:

$$u_j(r_j, \theta_j) = \sum_{m=1}^{\infty} a_{jm} r_j^m \sin m\theta_j + \frac{r_j^2}{4}[\cos 2\theta_j - 1] \tag{11-a}$$

- As for the six rectangular trapezoidal subdomains:

$$u_m(r_m, \theta_m) = \sum_{p=1}^{\infty} a_{mp} r_m^{\frac{4p}{3}} \sin(\frac{4p\theta_p}{3}) + \frac{r_m^2}{4}[\cos 2\theta_m - \sin 2\theta_m - 1] \tag{12-a}$$

Coefficients used in various auxiliary solutions are arbitrary constants. It is important to note that the thirty seven problems are not 'well posed' since the uniqueness of their solution is not assured. This is due to the fact that each Γ_j is only one part of the boundary of the subdomain Ω_j. We can develop the solution of the initial problem thanks to the multiplicity of auxiliary solutions, or failing that, good approximations of this solution.

Step 3: Connecting auxiliary solutions.

The last step of the method is the connection of auxiliary solutions between them. Therefore, we have just to set the continuity of the function and its normal derivative all along sub-boundaries Γ_{ij} separating both subdomains Ω_i and Ω_j. In practice, unable to solve an infinite system, we should generally use just approximate solutions. On the one hand, the approximation derives from the fact that developments 9-a to 12-a should be limited to a finite number of terms and on the other hand, with few exceptions, the approximation derives from the imperfect connection.

Approximate solutions (9-b) to (12-b) are obtained by limiting series that operate in general solutions. The number of terms kept in each sum is chosen according to Tolley [14, 15] principle which aims at representing approximate solutions using functions whose degree must be as uniform as possible. This is achieved by keeping more terms in the subdomains with the largest openings. If N is the number of coefficients kept for an opening angle $\pi/2$, the highest common divisor of the opening angles of 37 singular or pseudo singular vertices is 45º. For the first approximation, we keep two coefficients for 90º angles, three coefficients for 135º angles and so on, giving on the whole 140 coefficients. The total number of coefficients a_{kl} kept for all subdomain is $(12\times 2+6\times 3+8\times 4+11\times 6)N=140N$.

Therefore, the following approximate solutions are obtained:

- As for L-shaped domains

$$u_k(r_k,\theta_k)=\sum_{l=1}^{6N}a_{kl}r_k^{\frac{2k}{3}}\sin(\frac{2l\theta_k}{3})+\frac{r_k^2}{12\pi}[(3\pi-4\theta_k)\cos 2\theta_k-3\pi-4\log r_k\sin 2\theta_k] \quad (9\text{-b})$$

- As for squares

$$u_i(r_i,\theta_i)=\sum_{n=1}^{2N}a_{in}r_i^{2n}\sin 2n\theta_i+\frac{r_i^2}{4\pi}[(\pi-4\theta_i)\cos 2\theta_i-\pi-4\log r_i\sin 2\theta_i] \quad (10\text{-b})$$

- As for rectangles

$$u_j(r_j,\theta_j)=\sum_{m=1}^{4N}a_{jm}r_j^m\sin m\theta_j+\frac{r_j^2}{4}[\cos 2\theta_j-1] \quad (11\text{-b})$$

- As for trapezoids

$$u_m(r_m,\theta_m)=\sum_{p=1}^{5N}a_{mp}r_m^{\frac{4p}{3}}\sin(\frac{4p\theta_p}{3})+\frac{r_j^2}{4}[\cos 2\theta_m-\sin 2\theta_m-1] \quad (12\text{-b})$$

Then, we align auxiliary solutions in terms of the least squares, i.e. we set coefficients a_{kl} that allow minimizing the function.

$$I(a_{mn})=\sum_{i<j}\int_{\Gamma_{ij}}\left[(u_i(a_{ik})-u_j(a_{jl}))^2+\left(\frac{\partial u_i(a_{ik})}{\partial n_i}+\frac{\partial u_j(a_{jl})}{\partial n_j}\right)^2\right]ds_{ij} \quad (13)$$

Since n_i is the external normal to the subdomain Ω_i.

These coefficients a_{kl} are therefore solutions of the algebraic system with positive square matrix of $140\times N$ equations with $140\times N$ unknowns conventionally called Gauss' normal equations.

$$\frac{\partial I(a_{mn})}{\partial a_{kl}} = 0 \qquad (14)$$

For each subdomain, the global error defined in (15) decreases exponentially according to N approximation order, i.e. according to the total number of coefficients a_{kl} kept in series related to singularities, i.e. $140\times N$, Fig. 2.

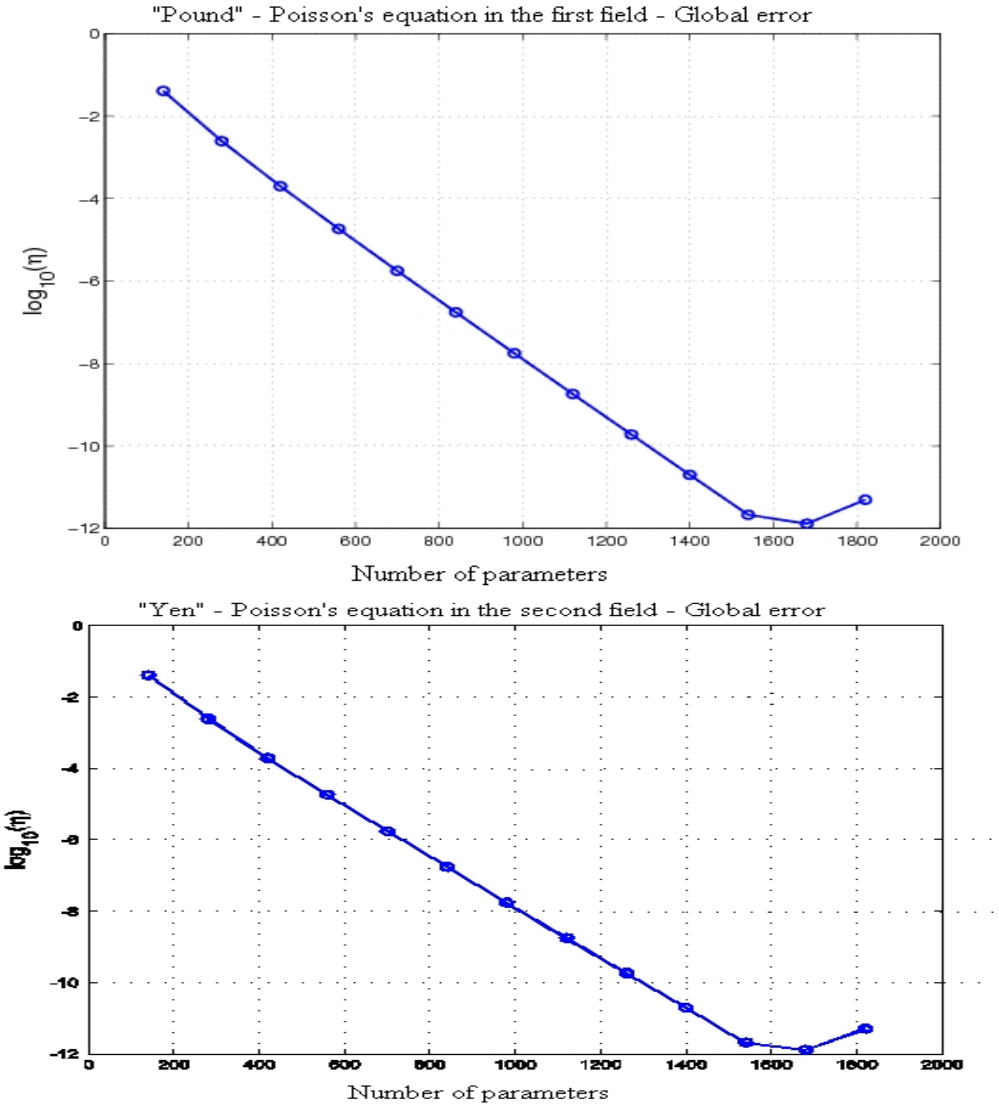

Fig. 2. Gordon Webb and Wolpert "Pound" and "Yen" isospectral domains. Evolution of the global error

$$\eta = \sum_{k<l} \frac{1}{S_{kl}} \int_{\Gamma_{kl}} \left[(u_k - u_l)^2 + \left(\frac{\partial u_k}{\partial \upsilon_k} + \frac{\partial u_l}{\partial \upsilon_l} \right)^2 \right] ds_{kl} \quad (15)$$

where ds_{kl} is the element which arch is Γ_{kl}, S_{kl} its length, ν_k and ν_k the normals to the sub-border separating both adjacent sub domains.

3. RESULTS AND DISCUSSION

For each of both membranes, the minimum global error is 1.3×10^{-12}. It is obtained at the twelfth approximation when $140 \times N = 1680$ coefficients a_{kl} are maintained as a whole. This suggests that the distorted u of the membrane can be determined with 13 or 14 significant digits, while its derivatives $\frac{\partial u}{\partial x}$ and $\frac{\partial u}{\partial y}$ may be calculated with 11 or 12 significant digits.

Points P_1 to P_4 shown in Fig. 1 will be used as control points to illustrate local convergence of our numerical results and compare them with those obtained using finite element method. These four points are located in the intersection of four sub-boundaries, i.e. in domains far from singularities, where the results obtained through large singular finite elements method are supposed to be the least accurate.

We applied the finite element method on five grids increasingly tight. Elements used are Lagrange quadratic elements and the automatic meshing has led to systems with 658; 2,115; 8,149; 31,977 and 126,673 equations for the first Gordon, Webb and Wolpert membrane and for systems 560, 2,083, 31,465 and 124,625 equations for the second Gordon, Webb and Wolpert membrane.

The first graphs (Fig. 3) show the evolution of the value of the function u in control points P_i according to the number of approximation N. Diagrams are semi-logarithmic and the local error is defined by (16)

$$\varepsilon = f_{ref} - f_{appx} \quad (16)$$

where f_{appx} is an approximate value and f_{ref} a reference value supposedly “exact”.

We took the solution obtained by the twelfth approximation of the large singular finite elements method as the reference, while maintaining a total number of 1,680 coefficients a_{kl} which are accurate to nearly 10^{-12}.

Curves containing the square markers correspond to approximations of finite element method and those containing circular markers dealt with large singular finite elements method. Square markers were evenly distributed on N scale while circles correspond to the entire values of N. The correlation between local absolute errors and the total error is highlighted by the dotted line curve which shows the evolution of the total error. As regards the large singular finite elements method, the ratio of 10^2 between the global

error and that shows that local values of the function u are obtained with accurate figures with $p+2$ accurate digits when the global error is about 10^{-p}.

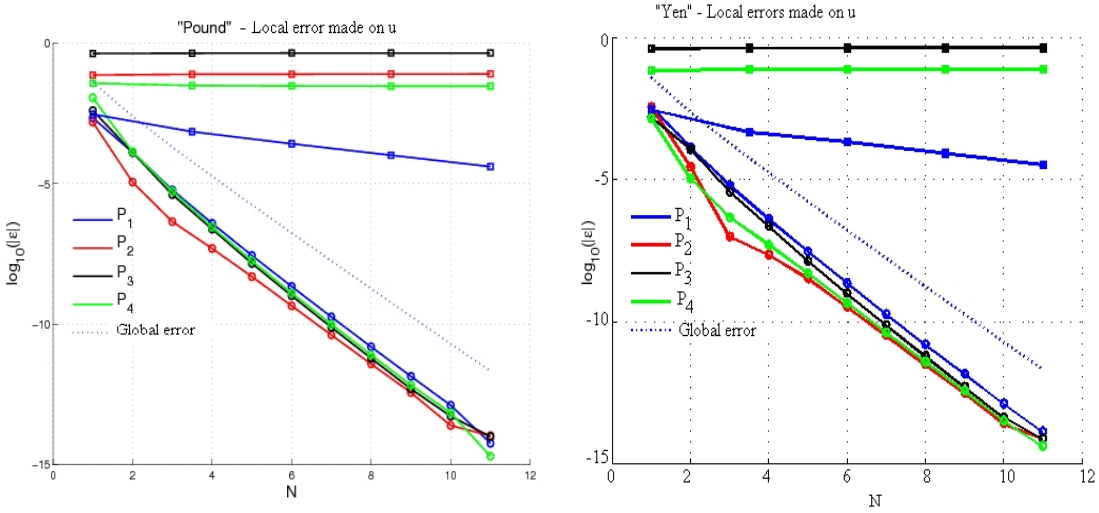

Fig. 3. Gordon Webb and Wolpert "Pound" and "Yen" isospectral areas. Local errors made on u in reference points. Comparison with finite elements method

We find that large singular finite elements method is much more accurate than the finite element method. Indeed, for the best approximations provided by both methods, the ratio between local error obtained with the finite element method and that obtained with large singular finite element method is about 10^{10} in P_1 and more than 10^{12} for other control points.

Diagrams in Figs. 4 and 5 are similar to those of Fig. 3. But they focus on comparing derivatives $\frac{\partial u}{\partial x}$ and $\frac{\partial u}{\partial y}$ in reference points P_i.

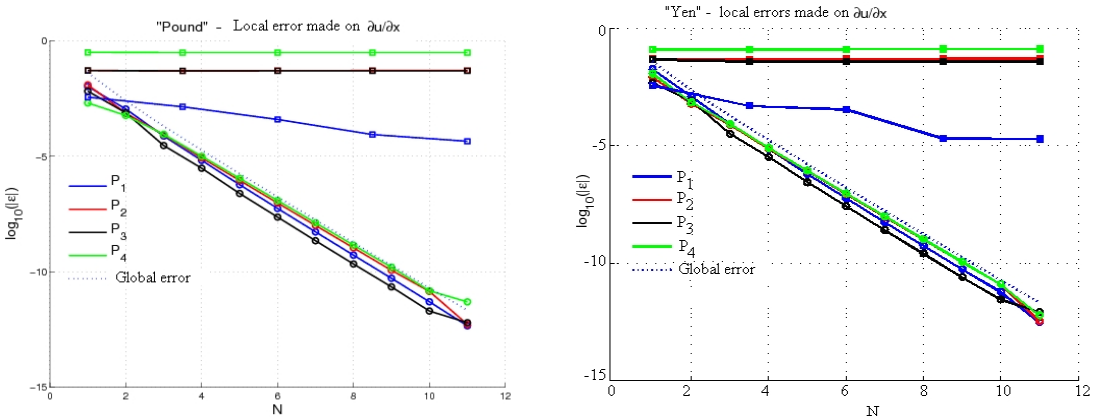

Fig. 4. Gordon Webb and Wolpert "Pound" and "Yen" isospectral domains. Local errors made on $\frac{\partial u}{\partial x}$ in reference points. Comparison with finite elements method

Conclusions that can be drawn are similar to those deduced from Fig. 3, while noting, however, that the curve reflecting the global error is closer to the curves of local errors (at least concerning the large singular finite elements method). This shows that local errors made with derives of function u almost the same as the global error. The accuracy of approximate values of the derivative is therefore lower than those of the function u. To conclude the study on Gordon, Webb and Wolpert membranes, some figures are submitted showing a planar view of the distorted u of the membrane (Fig. 6) along with level curves of u and of the magnitude of gradient $|\Delta u|$ (Fig. 7).

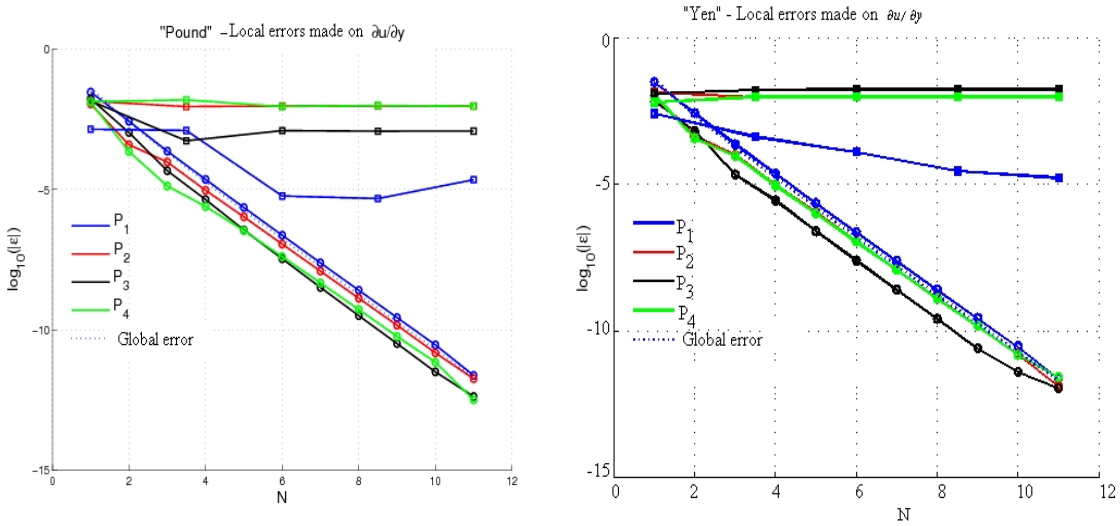

Fig. 5. Gordon Webb and Wolpert "Pound" and "Yen" isospectral domains. Local errors made on in reference points. Comparison with finite elements method

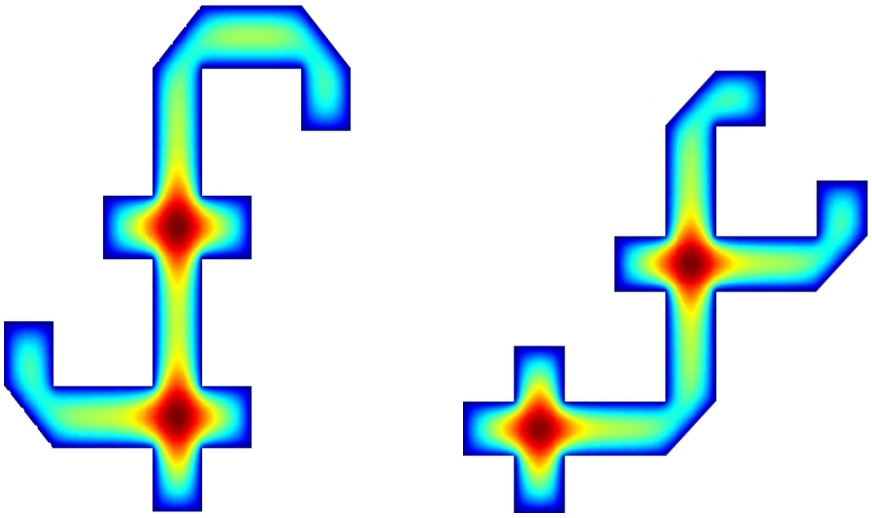

Fig. 6. Gordon Webb and Wolpert "Pound" and "Yen" isospectral domains. Planar view of the distorted u.

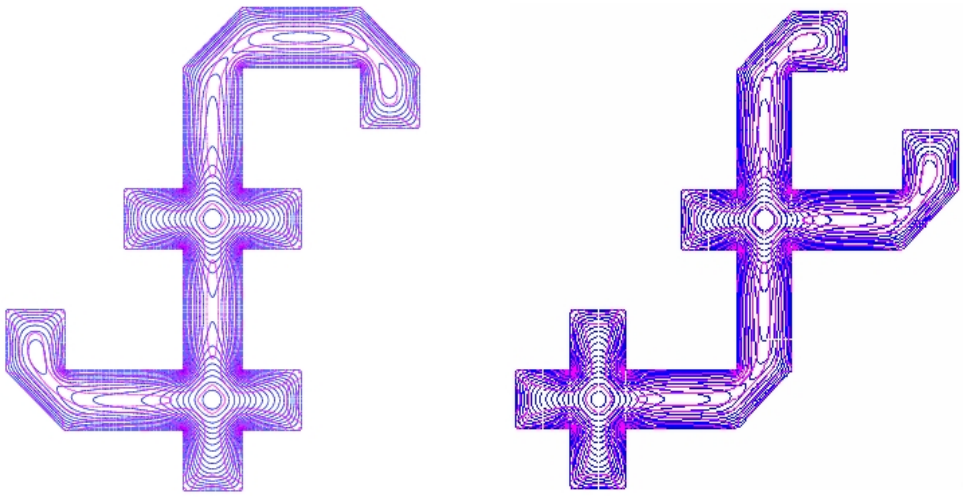

Fig. 7. Gordon Webb and Wolpert "Pound" and "Yen" isospectral domains. Level curves of u (in blue) and of $|\Delta u|$ (magenta)

In this study, we consider the large singular finite element method (LSFEM) using integration on interelements. This operation can be avoided using boundary collocation method as discussed by Kolodziej and Zielinski [16].

LSFEM can be also used to solve the eigenvalue problem for the Laplace operator, Descloux and Tolley [17]. A numerical study of the phenomenon of eigenvalue avoidance is developed by Betcke and Trefeten [18] which achieved the same or better accuracy with a simpler approach.

4. CONCLUSION

Large singular finite elements method gives very good results for both singularities and points located far from them. Its application provides a very low global error with a very low number of retained coefficients. Solutions to various problems are found in the analytical form, which provides all derivative values with the same accuracy as the basic values, without further formulation. By comparing results obtained with the conventional finite element method, this reveals the advantage for those obtained through large singular finite elements method, since it gives much more accurate results, especially around singularities where the finite element method gives unsatisfactory results.

COMPETING INTERESTS

There are no competing interests in this work.

REFERENCES

1. Barnill RE, Whiteman JR. Singularities due to re-entrant boundaries in elliptic problems. In L. Collatz (edn.) I.S.M.N. Birkhauser. 1977;19:29-45.
2. Emery AF. The use of singulary programming in finite difference and finite-element computations of temperature. Trans. ASME (C). 1973;95:344-351.

3. Fix GJ. Higher-order Raleigh-Ritz approximations. J. Math. Mech. 1969;18:645-647.
4. Motz H. The treatment of singularities of partial equations by relaxation methods. Quart. Appl. Math. 1946;4:371-377.
5. Strang G, Fix GJ. Analysis of the finite element method. Prentice Hall.1973.
6. Wait R., Mitchell AR. Corner singularities in elliptic problems by finite element methods. J. Comp. Phys. 1971;45-52. doi:10.1016/0021-9991(71)90033-7.
7. Kolodziej JA, Fraska A. Elastic torsion of bars possessing regular polygon in cross-section using BCM. Computers Structures. 2005;84:78-91.
8. Hassenpflug WC. Torsion of uniform bars with polygon cross section. Computers and mathematics with applications. 2003;46:313-392.
9. Zongo OM, Kam S, Ouedraogo A. Torsion of bars with regular polygonal sections. GJPAS. 2012;18(1-2):75-85.
10. Zongo OM, Kam S, Palm K., Ouedraogo A. Determining of temperature field in a L-shaped domain. Adv. Appl. Sci. Res. 2012;3(3):1572-1581.
11. Gordon C, Webb DL, Wolpert S. One cannot hear the shape of a drum. Bulletin of the American Society, 1992;27:134-138.
12. Landau L, Lifshitz E. Theory of elasticity. Edn Mir, Moscow; 1967.
13. Timoshenko SP, Goodier JH. Theory of elasticity, New York, McGraw Hill; 1970.
14. Tolley M. Grands éléments finis singuliers, Thèse de doctorat, Université Libre de Bruxelles, 1977. (French).
15. Tolley MD. Torsion des barres polygonales. Bull. Cl. Sc. 5ème série, 1977;LXIII(11):902-912. (French).
16. Kolodziej JA, Zielinski AP. Boundary collocation techniques and their application in ingeneering, WTT Press, Southampton; 2009.
17. Descloux J, Tolley MD. Approximation of the Poisson Problem and of the Eigenvalue Problem for the Laplace Operator by the Method of the Large Singular Finite Elements. Research Rept. Seminar für Angewandte Mathematik. 81-01, ETH Zürich; 1981.
18. Betcke T, Trefeten LN. Reviving the method of particular solutions. SIAM Review. 2005;47(3):469-491.

Peer-review history:
The peer review history for this paper can be accessed here:
http://www.sciencedomain.org/review-history.php?iid=168&id=4&aid=780